Comparison of Ring shear cell simulations in 2d/3d with experiments

Stefan Luding

Particle Technology, Nanostructured Materials, DelftChemTech, TU Delft,
Julianalaan 136, 2628 BL Delft, The Netherlands
e-mail: s.luding@tudelft.nl

Abstract

We present experiments together with corresponding molecular dynamics (MD) simulations of a two-dimensional (2D) and a three-dimensional (3D) granular material in Couette shear cells undergoing slow shearing. In 2D, the grains are disks confined between an inner, rotating wheel and a fixed outer ring. In 3D, the particles are disks, and a part of the bottom is rotating with the inner ring. The simulation results are compared to experimental studies and quantitative agreement is found within about 80-90 per-cent. Tracking the positions and orientations of individual particles allows us to obtain also density distributions, velocity- and rotation-rates in the system. The key issue is to show in how far quantitative agreement between an experiment and MD simulations is possible, besides the fact that many differences in model-details and the experiment exist.

We discuss the quantitative agreement/disagreement, give possible reasons, and outline further research perspectives. Especially the issue of a micro-macro transition will be detailed: Stress, strain, and other continuum quantities can be obtained from the microscopic simulations, showing that the granular material is compressive, anisotropic and micro-polar - all at the same time.

1. Introduction

For granular materials, the particle properties and interaction laws are inserted into a discrete particle molecular dynamics (MD), which then follows the evolution of the the dissipative many-particle system. From the discrete picture, the goal is to obtain continuum constitutive relations as needed for industrial design. Therefore, methods and tools to perform a so-called micro-macro transition [1–3] are used, with molecular dynamics simulations, as used here, as the basis. The "microscopic" simulations of a small samples (representative volume elements) are used to derive macroscopic constitutive relations needed to describe the material within the framework of a continuum theory.

Since every simulation relies on experiments for validation, in the following, two- and three-dimensional ring-shear test simulations will be compared to experimental results.

1.1. The Soft Particle Molecular Dynamics Method

Information about the behavior of granular media can be obtained from molecular dynamics (MD) or discrete element model (DEM) [1, 4–7]. Note that both methods are identical in spirit, however, different groups of researchers use these (and also other) names. Conceptually, the MD or DEM method has to be separated from the hard sphere event-driven (ED) molecular dynamics, and also from the so-called Contact Dynamics (CD). Alternative methods like cell-models or lattice gas methods are not discussed here.

1.2. Discrete Particle Model

The elementary units of granular materials are mesoscopic grains which deform under stress. Since the realistic modeling of the deformations of the particles is much too complicated, we relate the interaction force to the overlap δ of two particles. Note that the evaluation of the inter-particle forces based on the overlap may not be sufficient to account for the inhomogeneous stress distribution inside the particles. Consequently, our results presented below are of the same quality as the simple assumptions about the force-overlap relation [5, 8] Instead of descibing contact force laws in detail, we refer to the literature [6–8].

If all forces $\boldsymbol{f}_i$ acting on the particle i, either from other particles, from boundaries or from external forces, are known, the problem is reduced to the integration of Newton's equations of motion for the translational and rotational degrees of freedom. The equations of motion are thus a system of $\mathcal{D} + \mathcal{D}(\mathcal{D}-1)/2$ coupled ordinary differential equations to be solved in $\mathcal{D}$ dimensions. With tools from numerical integration, as nicely described in textbooks as [9, 10], this is a straightforward exercise. The typically short-ranged interactions in granular media, allow for a further optimization by using linked-cell or alternative methods in order to make the neighborhood search more efficient.

2. 2D Couette ring shear cell

The physical system discussed here was originally studied experimentally and numerically by various authors [11–13]. In the following, the experimental set-up is reviewed, similarities and differences between the simulations and the physical system are discussed, the initial conditions and the steady state are examined, and the results concerning the velocity field are presented.

2.1. Experimental Setup and Procedure

The experimental setup and results are discussed in more detail in Refs. [5, 11, 14, 15]. The apparatus, as sketched in Fig. 1, consists of (A) an inner shearing wheel (with radius $R = 10.32\,\mathrm{cm}$), and (B) an outer, stationary ring with radius $R_o = 25.24\,\mathrm{cm}$ confined by (C) planetary gears. In the experiments, a bimodal distribution of disks (D) is used, with about 400 larger disks of diameter 0.899 cm, and about 2500 smaller disks of diameter 0.742 cm. An inhomogeneous distribution is useful, since it limits the formation of hexagonally ordered regions over large scales, even though there might still be some short range order [16]. We use the diameter, $d = d_{\mathrm{small}}$, of the smaller disks as a characteristic length scale throughout this study.

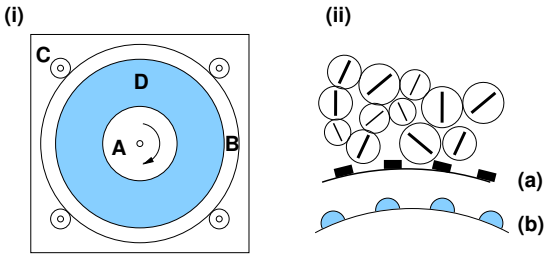

Figure 1.
(i) Schematic top view of the experimental setup.
(ii) schematic drawing of the disks close to the shearing wheel.
(**a**) experimental realization of the walls.
(**b**) realization of the walls in the simulation.

The experimental walls are fixed, corresponding to a *constant volume boundary condition*. All particles are inserted into the system and the shear is applied via the inner wall for several rotations, before averages in the nominally steady state are taken. If not explicitly mentioned, averages in the simulations are performed after about three rotations starting at $t = 180\,\mathrm{s}$, and extending over three rotations, until $t = 360\,\mathrm{s}$.

The mean packing fraction $\bar{\nu}$ (fractional area occupied by disks) is varied over the range $0.797 \leq \bar{\nu} \leq 0.837$ in the simulations. Note that the effect of the wall particles for the calculation of the global packing fraction is very small. For computing the packing fraction in the simulations, only half the volume of the small particles glued to the side walls is counted, so that these boundary particles always contribute $\bar{\nu}_{\mathrm{wall}} = 0.0047$ to $\bar{\nu}$. Taking or leaving a small or large particle leads to a density change of 0.00026 or 0.00038, respectively. The densities (area fractions) given have three digit accuracy in order to allow a distinction between runs differing by only a few particles. However, the error in the experimental density values is much larger (at least ± 0.02) due to the

following facts:
(i) the disks are not perfect in shape and diameter since they are cut out of a 6mm sheet of the material, (ii) the disks can tilt out of the horizontal thus enhancing the effective density, (iii) the disks are soft and thus compressible so that shape change may play some role, and (iv) the boundaries of the system are not perfect. Thus all density data have, for practical and experimental purposes, an absolute uncertainty of at least 0.02.

The shearing rate is set by Ω, the rotation rate of the inner wheel. A variation of Ω over $0.0029\,\mathrm{s}^{-1} \leq \Omega \leq 0.09\,\mathrm{s}^{-1}$ in the experiments shows rate independence in the kinematic quantities, except for some small, apparently non-systematic variations with Ω. A few simulations with $0.01\,\mathrm{s}^{-1} \leq \Omega \leq 1.0\,\mathrm{s}^{-1}$ also showed clear rate independence for the slower shearing rates.

2.2. Simulation Method and Similarity to the Experiment

Details of the simulations have been presented elsewhere [17], and we will not repeat these. The parameters used in the model were chosen to match the experiments as reasonably as possible. Specifically, the radii, static friction coefficient and density of the particles, and the size of the container match the experimental values. The boundary conditions are chosen to mimic those in the experiment, see Sec. 2.1. However, the "teeth" used on the inner and outer ring of the experiment are replaced by small disks with diameter d_{wall}, see Fig. 1.

As in the experiment, several packing fractions of the shear-cell are investigated in the simulations. For too low density, in the *sub-critical* regime, the particles are pushed away from the inner wall and lose contact, so that shearing stops. For too high densities, dilation and thus shear are hindered and the system becomes *blocked*, i.e. the inner particles slip on the inner wall and no shearband develops. The range of densities that allow for the steady state shear flow is extremely narrow.

Still, there remain some nominally modest differences between the experiment and the simulation, which may lead to differences between results for the two realizations. The main differences are:

- The numerical code used here only accounts for a very weak friction with the bottom plate, presumably smaller than reality. On the other hand, reduced friction in the experiment is achieved by powder on the bottom plate and this is not included in the simulations.
- Related to the disk shape of the particles is a possible small tilt of the real particles out of plane of observation, connected to increased tangential and frictional forces due to increased, artificial, normal forces.
- The particle-wall (and also the particle-particle) contacts are modeled by simple linear force laws and thus, possibly, do not reproduce reality to the extent desired.
- In the experiment the walls are never as perfectly round as in the sumulations, which in the end leads to a slightly larger effective radius of the inner wall and to

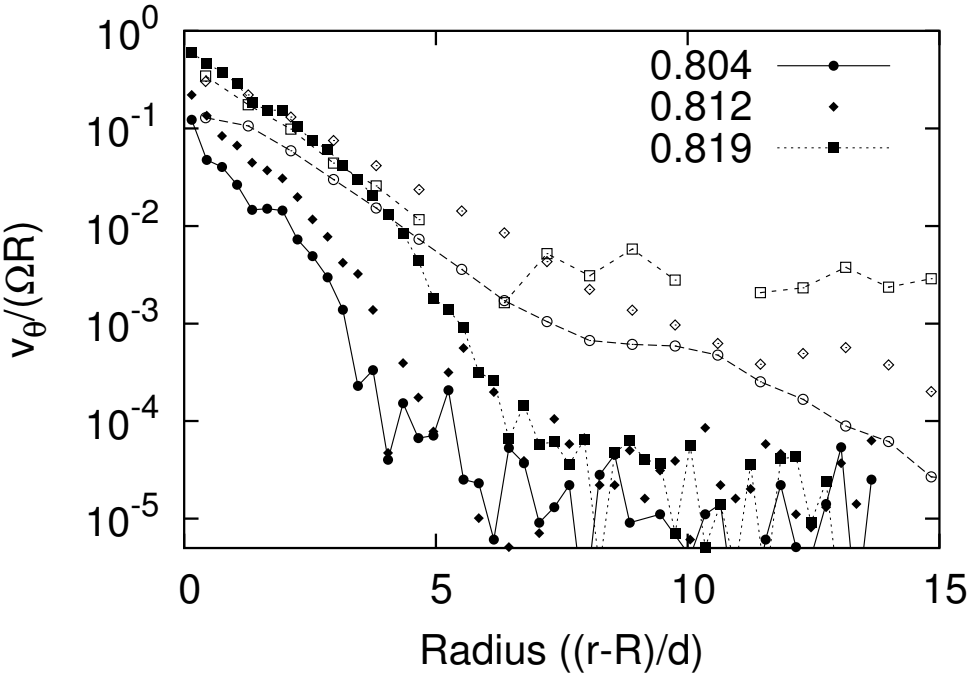

Figure 2. Velocity profiles for selected packing fractions $\bar{\nu}$. The solid and open symbols denote experimental and simulational data, respectively.

intermittency – sometimes nothing moves, until a bump in the wall finds particles to touch.

- The initial state is prepared differently for the experiments and the simulations. The starting state in the experiments is a nearly uniform density at the mean packing fraction, $\bar{\nu}$. The initial state of the simulation is an initially dilated state that is then compressed.

These factors apply for all the comparisons between the simulation and experimental data to follow. While there are differences in various details, many qualitative and quantitative results are in agreement for the experiment and simulation.

2.3. Velocity profiles

With varying density, the velocity profiles (and the spin profiles – not shown here) change also. In Fig. 2, data for the scaled velocity are shown for different $\bar{\nu}$, from both experiment and simulation. The profiles of $v_\theta/(\Omega R)$, show a roughly *exponential decay*, although there is some clear curvature in the experimental data at the outer edge of the shear zone, where the saturation level is reached. This *saturation level* of fluctuations in the velocity is at a higher level in the simulations, possibly due to the systematically larger shear rate in simulations used to save CPU-time, or due to the dubious model for bottom friction. However, the logarithmic scaling over-amplifies this very small difference.

Values of $v_0/(\Omega R) = 1$ would correspond to perfect shear in the sense that the particles are moving with the wall without slip. For high densities, the agreement between experiments and simulations is reasonable, but for low densities, the magnitude of the velocities differs strongly. This may be due to either the differences in bottom- or wall-friction, or due to more irregular and differently shaped walls in the experiments, causing more intermittency and thus reduced mean velocities.

The agreement in the velocity profiles is at least promising, given the various differences. Especially for higher densities, there is good quantitative agreement. Indeed, it is for this case that the bottom friction and wall effects are expected to be least important, since in this regime, the particle-particle interaction forces are at their strongest, and intermittent behavior is relatively unlikely.

When one examines the velocity- and spin-distributions in more detail, the data indicate (peaks near the origin) non-rotating particles at rest. These peaks become weaker with increasing density. Furthermore, the regions with negative spin and nonzero velocity grow with increasing density. This corresponds to a a concentration of probability for particles with non-slip motion of grains relative to the wheel. No-slip here means, that the particles execute a combination of backwards rolling and translation, such that the wheel surface and the disk surface remain in continuous contact.

In summary, both simulations and experiments show rate-independence within the statistical errors, and the range of rates that were studied. We have particularly focused on the dependence of the shearing states on the global packing fraction. Good agreement between simulation and experiment was found for the density profiles (modulo an overall density shift – data not shown here) associated with the formation of a shear band next to the inner shearing wheel with a characteristic width of about 5 to 6 particle diameters. Simulation and experiment also showed a roughly exponential velocity profile. However, the simulations did neither capture the density dependence of the experimental velocity profiles for small densities, nor some details of the shape, especially at the outer edge of the shear band. In this regard, further exploration of the role played by roughness of the shearing surface and the effect of the particle-bottom friction are necessary. The former can lead to more intermittent behavior, whereas the latter might explain the velocity-drop at the outer edge of the experimental shear band.

3. Ring shear cell simulation in 3D

The simulation in this section models a ring-shear cell experiment, as recently proposed [7, 18, 19]. The interesting observation in the experiment is a universal shear zone, initiated at the bottom of the cell and becoming wider and moving inwards while propagating upwards in the system.

3.1. Model system

The numerical model chosen here is MD with smooth particles in three dimensions. In order to save computing time, only a quarter of the ring-shaped geometry is simulated. The walls are cylindrical, and are rough on the particle scale due to some attached particles. The outer cylinder wall with radius R_o, and part of the bottom $r > R_s$ are rotating around the symmetry axis, while the inner wall with radius R_i, and the attached bottom-disk $r < R_s$ remain at rest. In order to resemble the experiment, the geometry data are $R_i = 0.0147\,\mathrm{m}$, $R_s = 0.085\,\mathrm{m}$, and $R_o = 0.110\,\mathrm{m}$. Note that the small R_i value is artificial, but it does not affect the results for small and intermediate filling heights.

The slit in the bottom wall at $r = R_s$ triggers a shear band. In order to examine the behavior of the shear band as function of the filling height H, this system is filled with 6000 to 64000 spherical particles with mean radius 1.0 mm and radii range 0.5 mm $< a <$ 1.5 mm, which interact here via repulsive and dissipative forces only. The particles are forced towards the bottom by the gravity force $\boldsymbol{f}_g = m\boldsymbol{g}$ here and are kept inside the system by the cylindrical walls. In order to provide some wall roughness, a fraction of the particles (about 3 per-cent) that are originally in contact with the walls are glued to the walls and move with them.

3.2. Material and system parameters

The material parameters for the particle-particle and -wall interactions are $k = 10^2\,\mathrm{N/m}$ and $\gamma_0 = 2.10^{-3}\,\mathrm{kg/s}$. Assuming a collision of the largest and the smallest particle used, the reduced mass $m_{12} = 2.94\,10^{-6}\,\mathrm{kg}$, leads to a typical contact duration $t_c = 5.4\,10^{-4}\,\mathrm{s}$ and a restitution coefficient of $r = 0.83$. The integration time step is $t_{\mathrm{MD}} = 5.10^{-6}\,\mathrm{s}$, i.e. two orders of magnitude smaller than the contact duration.

The simulations run for 25 s with a rotation rate $f_o = 0.01\,\mathrm{s}^{-1}$ of the outer cylinder, with angular velocity $\Omega_o = 2\pi f_o$. For the average of the displacement, only times $t > 10\,\mathrm{s}$ are taken into account. Within the averaging accuracy, the system seemingly has reached a quasi-steady state after about 8 s. Three realizations with different filling height are displayed in Fig. 3, both as top- and front-view.

3.3. Shear deformation results

From the top-view, it is evident that the shear band moves inwards with increasing filling height, and it also becomes wider. From the front-view, the same information can be evidenced and, in addition, the shape of the shear band inside the bulk is visible: The inwards displacement happens deep in the bulk and the position of the shear band is not changing a lot closer to the surface.

In order to allow for a more quantitative analysis of the shear band, both on the top and as function of depth, we perform fits with the universal shape function proposed in [18]:

$$\frac{v_\varphi(r)}{r\Omega_o} = A\left(1 + \mathrm{erf}\left(\frac{r - R_c}{W}\right)\right) \ , \tag{1}$$

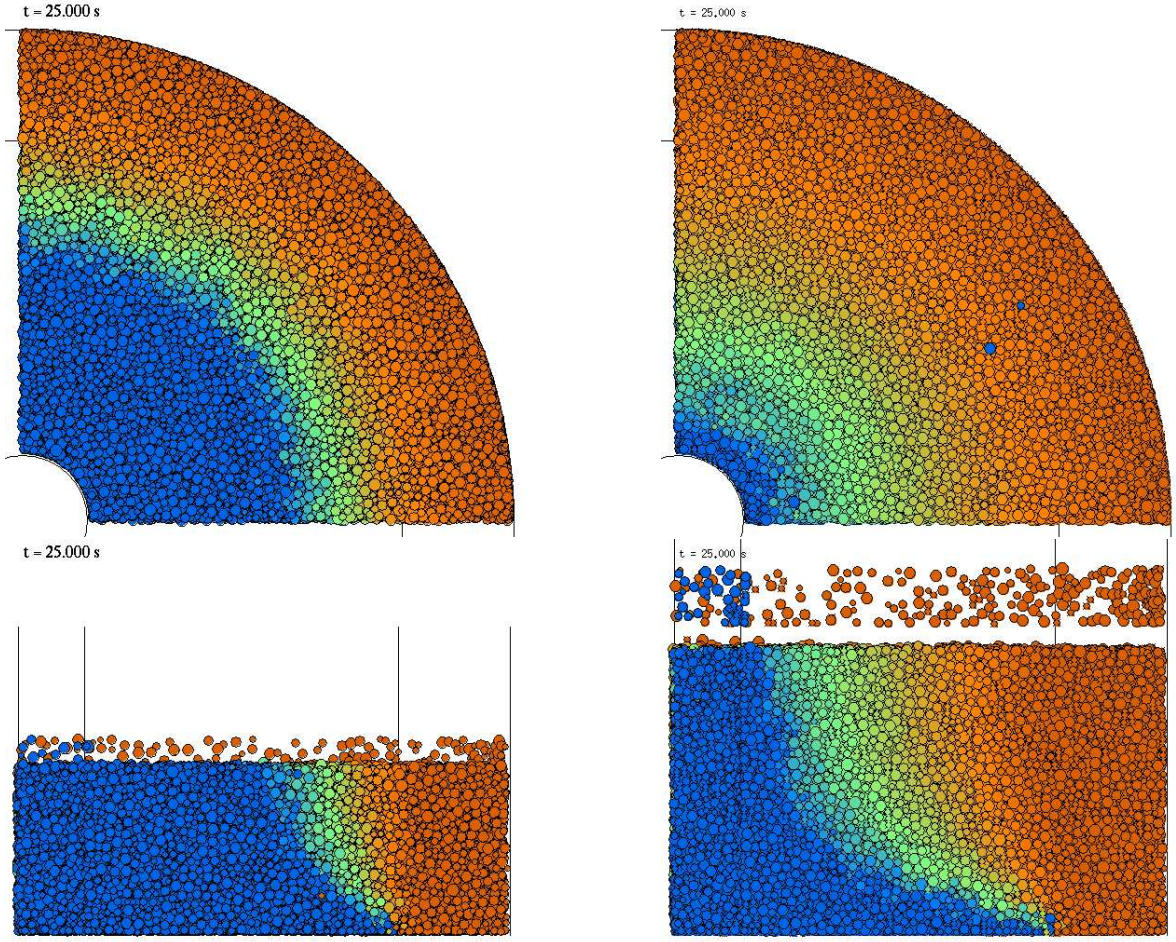

Figure 3. Snapshots from simulations with different filling heights seen from the top and from the front, and the particle numbers $N = 34518$ (Left) and $N = 60977$ (Right). The colors blue, green, orange and red denote particles with $r\,\mathrm{d}\phi \leq 0.5\,\mathrm{mm}$, $r\,\mathrm{d}\phi \leq 2\,\mathrm{mm}$, $r\,\mathrm{d}\phi \leq 4\,\mathrm{mm}$, and $r\,\mathrm{d}\phi > 4\,\mathrm{mm}$, i.e. the displacement in tangential direction per second, respectively. The filling heights in these simulations are $H = 0.037\,\mathrm{m}$, and $0.061\,\mathrm{m}$.

where A is a dimensionless amplitude $A = 0.50 \pm 0.02$, R_c is the center of the shearband, and W its width.

The fits to the simulations confirm the experimental findings in so far that the center of the shear band, as observed on top of the material, see Fig. 4, moves inwards with a $R_c \propto H^{5/2}$ behavior, and that the width of the shear band increases almost linearly with H. Quantitatively speaking, the agreement is 80%. For filling heights larger than $H \approx 0.05\,\mathrm{m}$, deviations from this behavior are observed, because the inner cylinder is reached and thus sensed by the shearband. Slower shearing does not affect the center position, but reduces slightly the width (checked only by one simulation).

Like in the experiments, the behavior of the shearband within the bulk, see Fig. 5, deviates qualitatively from the behavior seen from the top. Instead of a slow motion of

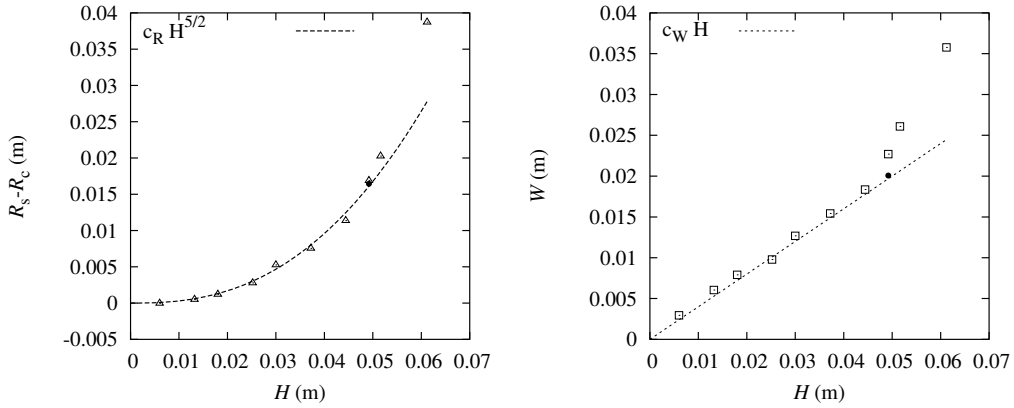

Figure 4. (Left) Distance of the top-layer shearband center from the slit, both plotted against the filling height H. The open symbols are simulation results, the solid symbol is a simulation with slower rotation $f_o = 0.005\,\mathrm{s}^{-1}$, and the line is a fit with constant $c_R = 30$. (Right) Width of the shearband from the same simulations; the line is a fit with $c_W = 2/5$.

the shear band center inwards, the shear band rapidly moves inwards at small heights h, and reaches a saturation distance with small change closer to the surface. Again, a slower rotation does not affect the center but reduces the width.

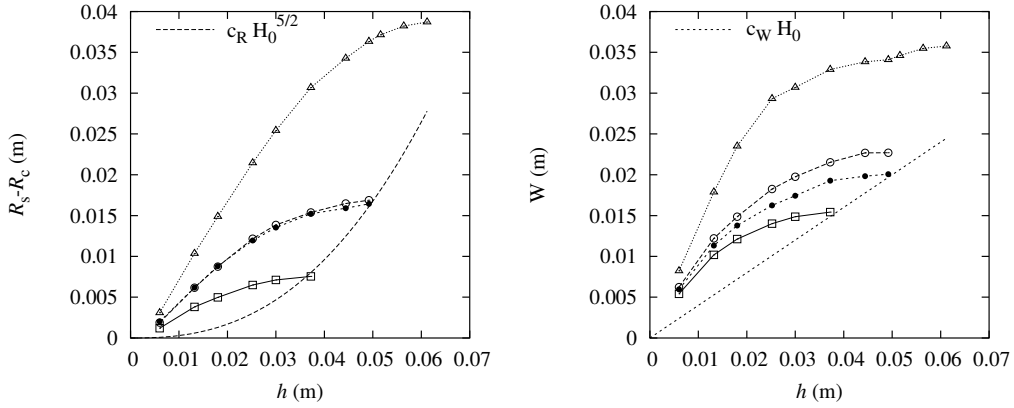

Figure 5. (Left) Distance of the bulk shearband center from the slit and, (Right) width of the shearband, both plotted against the height h. The open symbols are simulation results obtained with $f_o = 0.01\,\mathrm{s}^{-1}$, the solid symbols are obtained with slower rotation $f_o = 0.005\,\mathrm{s}^{-1}$. Squares, circles and triangles correspond to the filling heights $H = 0.037\,\mathrm{m}$, $0.049\,\mathrm{m}$, and $0.061\,\mathrm{m}$, respectively. The curves are identical to those plotted in Fig. 4.

3.4. Discussion

In summary, the example of a peculiar ring shear cell simulation in 3D has shown, that even without the more complicated details of fancy interaction laws, experiments can be reproduced quantitatively with 80% agreement. This is a promising starting point

for the challenge in the future: the micro-macro transition in 3D and the continuum theory formulation of the shear band problem.

4. Conclusion

Some examples of ring shear cell simulations in both 2D and 3D showed qualitative agreement with experiments. Even though the model is less involved than reality – many details as discussed above are not catched by the simulations – there is quantitative agreement in the denser regimes for both 2D and 3D. The error margin is about 20 per-cent.

In conclusion, molecular dynamics methods are a helpful tool for the understanding of granular systems because they allow insight on the particle and the contact level. The qualitative approach of the early years has now developed into the attempt of a quantitative predictive modeling of the diverse modes of complex behavior in granular media. This will eventually lead to elaborate constitutive models for quasi-static, dense systems with predictive value, e.g., for shear band localisation.

Acknowledgements

We acknowledge the financial support of several funding institutions that supported the reviewed research, the Deutsche Forschungsgemeinschaft (DFG), and the Stichting voor Fundamenteel Onderzoek der Materie (FOM), financially supported by the Nederlandse Organisatie voor Wetenschappelijk Onderzoek (NWO). Furthermore, also the helpful discussions with the many persons that contributed to these results are acknowledged.

References

[1] P. A. Vermeer, S. Diebels, W. Ehlers, H. J. Herrmann, S. Luding, and E. Ramm, editors. *Continuous and Discontinuous Modelling of Cohesive Frictional Materials*, Berlin, 2001. Springer. Lecture Notes in Physics 568.

[2] T. Pöschel and S. Luding, editors. *Granular Gases*, Berlin, 2001. Springer. Lecture Notes in Physics 564.

[3] J. G. Kirkwood, F. P. Buff, and M. S. Green. The statistical mechanical theory of transport processes. *J. Chem. Phys.*, 17(10):988, 1949.

[4] H. J. Herrmann, J.-P. Hovi, and S. Luding, editors. *Physics of dry granular media - NATO ASI Series E 350*, Dordrecht, 1998. Kluwer Academic Publishers.

[5] M. Lätzel, S. Luding, H. J. Herrmann, D. W. Howell, and R. P. Behringer. Comparing simulation and experiment of a 2d granular couette shear device. *Eur. Phys. J. E*, 11(4):325–333, 2003.

[6] S. Luding. Micro-macro transition for anisotropic, frictional granular packings. *Int. J. Sol. Struct.*, 41:5821–5836, 2004.

[7] S. Luding. Molecular dynamics simulations of granular materials. In H. Hinrichsen and D. E. Wolf, editors, *The Physics of Granular Media*, pages 299–324, Weinheim, Germany, 2004. Wiley VCH.

[8] S. Luding. Granular media: Information propagation. *Nature*, 435:159–160, 2005.

[9] M. P. Allen and D. J. Tildesley. *Computer Simulation of Liquids*. Oxford University Press, Oxford, 1987.

[10] D. C. Rapaport. *The Art of Molecular Dynamics Simulation.* Cambridge University Press, Cambridge, 1995.

[11] C. T. Veje, D. W. Howell, R. P. Behringer, S. Schöllmann, S. Luding, and H. J. Herrmann. Fluctuations and flow for granular shearing. In H. J. Herrmann, J.-P. Hovi, and S. Luding, editors, *Physics of dry granular media - NATO ASI Series E 350*, page 237, Dordrecht, 1998. Kluwer Academic Publishers.

[12] S. Schöllmann. Simulation of a two-dimensional shear cell. *Phys. Rev. E*, 59(1):889–899, 1999.

[13] H. J. Herrmann and S. Luding. Modeling granular media with the computer. *Continuum Mechanics and Thermodynamics*, 10:189–231, 1998.

[14] D. Howell, R. P. Behringer, and C. Veje. Stress fluctuations in a 2d granular Couette experiment: A continuous transition. *Phys. Rev. Lett.*, 82(26):5241–5244, 1999.

[15] D. W. Howell, R. P. Behringer, and C. T. Veje. Fluctuations in granular media. *Chaos*, 9(3):559–572, 1999.

[16] S. Luding. Liquid-solid transition in bi-disperse granulates. *Advances in Complex Systems*, 4(4):379–388, 2002.

[17] M. Lätzel, S. Luding, and H. J. Herrmann. Macroscopic material properties from quasi-static, microscopic simulations of a two-dimensional shear-cell. *Granular Matter*, 2(3):123–135, 2000. e-print cond-mat/0003180.

[18] D. Fenistein and M. van Hecke. Kinematics – wide shear zones in granular bulk flow. *Nature*, 425(6955):256, 2003.

[19] D. Fenistein, J. W. van de Meent, and M. van Hecke. Universal and wide shear zones in granular bulk flow. *Phys. Rev. Lett.*, 92:094301, 2004. e-print cond-mat/0310409.